Topological Considerations for a CONUS Deployment of CASA-Type Radars

Anthony P Hopf, David L Pepyne, and David J McLaughlin
Center for Collaborative Adaptive Sensing of the Atmosphere*
Electrical and Computer Engineering Department
University of Massachusetts, Amherst, USA

1. Introduction

Leveraging the computer chip and networking technologies that have benefited so much from Moore's law of increases in capabilities and cost reductions, the National Science Foundation Engineering Research Center (ERC) for Collaborative Adaptive Sensing of the Atmosphere (CASA) is transforming the way we do atmospheric sensing. In contrast to today's national scale atmospheric sensing radar systems which are based on small numbers of very large, very high-power, long-range radars that operate essentially as isolated units, CASA is engineering a technology based on a tightly integrated, densely packed network of small size, low power, short-range, solid-state radars with overlapping coverage for coordinated scanning and data fusion. Instead of radars with 10 m antenna, 100's of kW transmit power, and 100s of km spacing, CASA radars would be 1 m in size, have solid-state panels with transmit powers in the 10's of W, and spacing of 10s of km.

The close spacing of a CASA network "defeats" the blockage due to the curvature of the earth, which limits today's widely spaced radars from viewing weather hazards, aircraft, smoke, and chemical contaminants at the earth's surface. In addition, the diversity of multiple views at each location in the network greatly improves detection, resolution, and accuracy of the collected measurements for supporting multiple end-users and applications. Field tests being conducted by the CASA ERC are demonstrating dramatic improvements over the current state-of-the-art long-range paradigm. One such improvement is the ability to support the atmospheric boundary layer sensing needs of a diverse population of end-users ranging from operational forecasters, to emergency managers, to researchers McLaughlin et al. (2009).

Due to their very large size and very high-radiated power, long-range radars require dedicated land, towers, and other support infrastructure. Since the radars are relatively few in number, site selection is generally dictated by population density and proximity to other infrastructure such as airports Leone et al. (1989). As a result, coverage is highly non-uniform over the network due to earth curvature, terrain blockage, and the loss of resolution and power density related to beam spreading. The WSR-88D NEXRAD system in the United States, which represents the state-of-the-art in the traditional long-range radar paradigm, provides the best weather sensing capability in the world, with unquestioned socioeconomic value. The deficiencies that the NEXRAD system does have, such as insufficient low-level coverage, poor coverage in rough terrain, and insufficient resolution far from the radar, are due precisely to the wide-spacing and non-uniform deployment of the radars (NRC).

Many of the deficiencies of long-range radar systems, particularly their inability to see low level areas, can only be overcome through a more dense deployment of radars. This is illustrated in Figure 1, which plots the rela-

*This work is supported primarily by the Engineering Research Centers Program of the National Science foundation under NSF award number 0313747. Any opinions, findings, conclusions, or recommendations expressed in this material are those of the authors and do not necessarily reflect those of the National Science Foundation.

tionship between the denseness of a radar network and its low-altitude coverage. The vertical bars at 345 km and 230 km represent the average spacing between the radars in the NEXRAD system in the western and eastern U.S., respectively. This non-uniform density leaves the west with poorer coverage than the east. Even in the east, coverage in the lowest 100's of meters above ground level is very limited. The vertical bar on the left of Figure 1 shows CASAs 30 km radar spacing. This spacing represents a series of tradeoffs between low-altitude coverage, radar cost drivers (operating frequency, transmit power, antenna size, solid-state manufacturing technology), and system performance (sensitivity, resolution, update time) McLaughlin et al. (2009). The spacing also represents an increase in density over NEXRAD of more than 60:1, i.e., every NEXRAD would be replaced by 60 CASA-type radars; a replacement of 150 radars by 10,000.

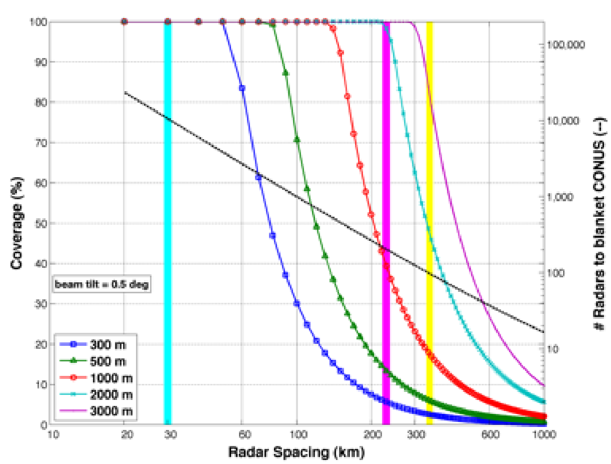

Figure 1: Percent coverage (colored lines) and number of radars needed for CONUS coverage (dashed line) as a function of the spacing between the radars in a network. The vertical bar at 345 km is the average spacing of the NEXRAD radars to the west of the Rocky Mountains, and the vertical bar at 230 km is the average spacing of the NEXRAD radars to the east of the Rocky Mountains. The vertical bar at 30 km is the representative spacing of the radars in the CASA IP1 testbed in Oklahoma. Figure taken from McLaughlin et al. (2009)

This paper discusses several of the key topological considerations in deploying a dense network of low power, short range, CASA-type radars. A key contribution is a presentation of the mathematics behind Figure 1, which was presented in (McLaughlin et al. (2009)) but without derivation. This is done in Sections 2 and 3. Figure 1 assumes a topology that places radars at the vertices of a uniform mesh of equilateral triangles. Section 4 presents the second contribution of this paper, which is an analysis of the effect of perturbing the triangular topology to a square topology. The square topology is investigated as a way to reduce beam steering related performance degradation in the paradigm shift from mechanically scanned radar technology to solid-state electronically scanned phased array radar (PAR) technology. The paper closes in Section 5 with a brief summary and mention of on-going work.

2. Coverage

Primary to any ground-based network of surveillance radars is consideration of coverage; how low, how high, and how complete in area. With respect to coverage, the spacing between the radars, R_{sp}, is the fundamental design parameter. This section is used to identify the layout, key mathematical relationships, and assumptions necessary to illustrating the impact R_{sp} has on network coverage. These mathematical relationships and assumptions will then be used to build the equations that govern Figure 1.

The basis of our analysis is the network topology in Figure 2. This topology, characterized by radars placed to form a uniform mesh of equilateral triangles with spacing R_{sp} between them, has some nice properties as discussed in (Brewster et al. (2005)) in terms of satisfaction of conditions for dual-Doppler wind vector retrieval (Wang et al. (2008)), and was the topology chosen for the four node IP1 testbed network deployed by CASA in southwestern Oklahoma (http:// socc.caps.ou.edu/).

In practice the mesh of equilateral triangles in Figure 2 is laid out on the surface of the earth over variable terrain. However, to emphasize the earth curvature problem, we will assume a smooth, spherical earth. Under a smooth earth assumption, our results are conservative in the sense that we ignore terrain blockage, but block-

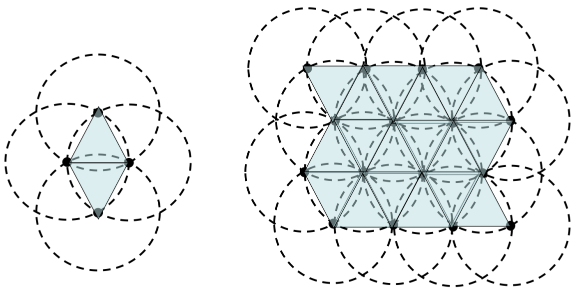

Figure 2: Network topology for a CASA-type dense radar network: radars with 40 km range placed 30 km apart to form a mesh of equilateral triangles. The network of the left is the basic topology of the CASA IP1 testbed network deployed in southwestern Oklahoma. The network on the right shows a larger four row, four column example.

age due to the curvature of the surface of the earth is still unavoidable.

The coverage by a network of ground-based, monostatic radars is determined by the union of the regions covered by the individual radars. Practical scanning limits in elevation produce a blind region directly above each radar. Under a smooth earth assumption, this blind region, termed the radars cone-of-silence, causes the coverage at any given height, h, to resemble a donut. However, since we are interested in small heights, h, and since for a CASA-type network we assume the radar maximum range $R_{max} \geq R_{sp}$, we can ignore the cone-of-silence, since either its area will be small compared to the total area covered by the donut, or it will be covered by a neighboring radar. In this case, the coverage by each radar at height, h when projected down onto the surface of the earth is a disk of radius s_h and the network coverage is a union of such disks. Regarding s_h, a rearrangement of the beam height equations from Doviak and Zrnić (1993) gives,

$$s_h = k_e a \sin^{-1}\left(\frac{r\cos\theta_{min}}{k_e a + h}\right) \tag{1}$$

where h is the height above ground level of interest, θ_{min} is the minimum antenna elevation tilt angle (θ_{min} = 0.5 for NEXRAD, 0.9 for CASA), k_e (typically taken as = 4/3) accounts for atmospheric refraction, a (= 6371 km) is the radius of the earth, and,

$$r = min\big[\sqrt{h^2 + 2hk_e a + (k_e a \sin\theta_{min})^2} - k_e a \sin\theta_{min}, R_{max}\big] \tag{2}$$

where R_{max} is the maximum range of the radar (R_{max} = 230 km for NEXRAD, 40 km for CASA).

a. *Low-Level Coverage*

To calculate the percent coverage at height, h, above ground level as a function radar spacing, R_{sp}, for a network of radars arranged in an equilateral triangle topology it suffices to consider a single unit cell and the three cases identified in Figure 3. The sufficiency of extrapolating network coverage from the coverage of a single triangular unit cell follows from the fact that, under the smooth earth assumption, both the size of each triangular unit cell and the size of each radar coverage disk is the same for each unit cell and each radar.

The coverage for each of the three cases in Figure 3 is given in the equation below: the first row corresponding to case (a) in the figure, the second row to case (b), and the third row to case (c).

$$C(h) = 100 \times \begin{cases} \frac{2\pi s_h^2}{\sqrt{3}R_{sp}^2} & 0 \leq s_h < \frac{R_{sp}}{2} \\ \frac{0.5\pi s_h^2 - 1.5 s_h^2(\phi - \sin\phi)}{0.25\sqrt{3}R_{sp}^2} & \frac{R_{sp}}{2} \leq s_h < \frac{R_{sp}}{\sqrt{3}} \\ 1 & \frac{R_{sp}}{\sqrt{3}} \leq s_h \end{cases} \tag{3}$$

where s_h is calculated using equation 1 and,

$$\phi = 2\cos^{-1}\left(\frac{R_{sp}}{2s_h}\right) \tag{4}$$

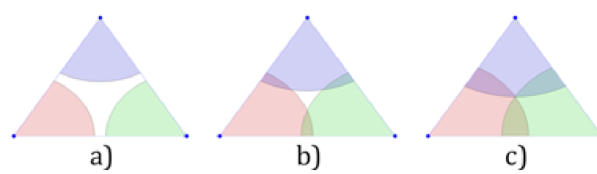

Figure 3: Three cases for calculating coverage percentage for a single triangular unit cell.

3. Number of Radars

The previous section showed that the only way to defeat the earth curvature problem, so as to probe the lowest reaches of the atmospheric boundary layer, is to reduce the spacing between the radars. Closer more dense spacing obviously requires more radars to cover a given domain. This section presents the equation for the number of radars required to cover a domain of a given size as a function of radar spacing, R_{sp}. Specifically, the domain of interest is the Contiguous United States (CONUS), estimated as a square with sides 2843 km x 2843 km. Taking the area covered by the network as the sum of the areas of the triangular unit cells, equation 5 gives the number of radars needed to cover the CONUS.

$$N_r = \left(ceil \left[\frac{2843}{\frac{\sqrt{3}}{2} R_{sp}} \right] + 1 \right) \left(ceil \left[\frac{2843}{R_{sp}} \right] + 1 \right) \quad (5)$$

Where $ceil$ is the ceiling function (round up to the nearest integer). The dotted black line in Figure 1 is obtained directly from equation 5 above.

4. Perturbation from a Triangle

The coverage results presented in the previous sections are predicated on the antenna being able to tilt to angles of 30 degrees or more in elevation. With a narrow pencil a desire for fast temporal updates prohibits the sit-and-spin scan strategy used by traditional surveillance radars such as NEXRAD. To achieve fast temporal updates and to service the data needs of multiple end-users and multiple applications, CASA has introduced the concept of radar operations termed Distributed Collaborative Adaptive Sensing (DCAS) (McLaughlin et al. (2005)). At its heart, DCAS is a beam scheduling technique designed primarily to trade-off sample rates against data utility to end-users and secondarily to coordinate beam crossing times, crossing angles, and so on for network-based data fusion algorithms such as dual-Doppler wind vector retrieval (Wang et al. (2008)).

The need to deploy 10,000 radars and the need for DCAS scanning to improve temporal resolution and to serve the data needs of multiple end-users and applications points to the need for a small, easily mounted, low-cost, highly reliable, and very agile radar technology. While CASAs field test trials so far have used mechanically scanned parabolic dish radars, the ERC is working with its partners to develop a small X-band PAR technology for a CASA-type deployment (McLaughlin et al. (2009); Salazar et al. (2008); Hopf et al. (2009)). The solid-state flat panel design of such radars give them advantages over mechanically scanned radars in terms of reliability and mounting; as they can be placed on the sides of existing infrastructure elements such as buildings and telecommunication towers, whereas a mechanically scanned radar typically has to be mounted on the top of a structure for a full unobstructed 360 degree view.

In a PAR deployment, coverage is just one of the considerations that needs to be addressed in choosing the most appropriate network topology. With a PAR the flat panel antenna itself remains fixed while the beam is pointed electronically. As a PAR beam is steered a number of things occur that degrade performance: the beam width gets wider and the antenna gain goes down (Mailloux (2005)). These two characteristics limit practical beam steering from a PAR panel to about 60 degrees to either side of boresight. As a result, a surveillance application would therefore require at least 3 panels per radar site for full 360 degree coverage. An additional characteristic of PAR that has just recently come to light has to do with PAR polarimetry. Because raindrops tend to flatten from spherical to oblate spheroids as they fall, their scattering characteristics in the horizontally polarized dimension differ from their scattering characteristics in the vertically polarized dimension. This asymmetry in scattering can be used for hydrometeor classification leading among other things to improved quantitative precipitation estimation (QPE) and in short-wavelength X-band radars, such as a CASA-type radar, to algorithms for attenuation estimation and correction (Liu et al. (2007)). To exploit these polarimetry advantages, the mechanically scanned radars in the CASA IP1 network are dual-pol, and the PAR that the CASA ERC is developing will also be dual-pol. The difficulty with dual-pol PAR is that, unlike a mechanically scanned radar, when a polarimetric PAR beam is steered, the alignment of the polarizations changes relative to the horizontal and vertical dimensions of the raindrops (Zhang et al. (2008)). When this happens the radar is no longer accurately measuring the drop shape asymmetry and errors will be introduced into the dual-pol variables, Z_{dr} being particularly sensitive (Wang et al. (2005)). The main consequence of this property of PAR is a potential further reduction in the beam steering limits. Clearly any reduction in the beam steering limits below 60 degrees requires an additional panel at each site; a 45 degree beam steering limit requiring 4 panels at each site.

Once beam steering limits are imposed it becomes necessary to understand the interaction between number of panels, the relative orientations of the panels at the different sites, and network performance measures such as the ability to perform attenuation correction, network-based reflectivity retrievals, and dual-Doppler wind field measurements. A preliminary investigation was started in (Salazar and McLaughlin (2007); Hopf et al. (2008)) where the two topologies and panel arrangements shown below in Figure 4 were compared.

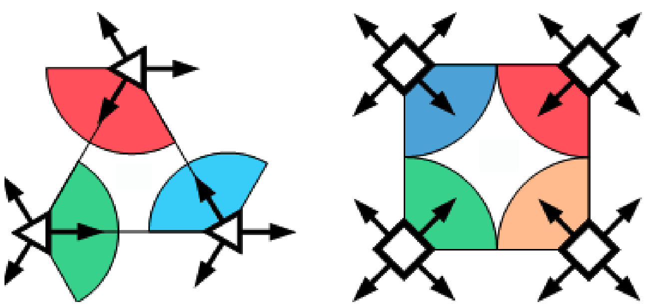

Figure 4: Competing topologies for a deployment of polarimetric PAR; triangular topology with 3 PAR panels per radar site (left) and square topology with 4 PAR panels per radar site (right).

In light of the above, it is necessary to explore what happens to coverage when we perturb the shape of the unit cells away from the perfect equilateral triangle topology. Specifically, consider arranging the radars into a mesh of squares of size R_{sp} by R_{sp}. As shown in Figure 5, one way to view this square topology is as a perturbation of the equilateral triangle topology into two back-to-back isosceles triangles with two sides equal in length to R_{sp}, and the third side equal in length to $\sqrt{2}R_{sp}$.

Following the same procedure used in Sections 2 and 3 we can obtain a plot similar to Figure 1 for the case

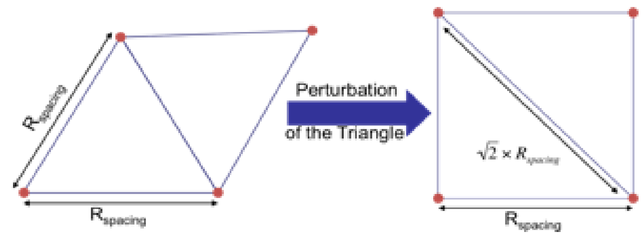

Figure 5: Square topology as a perturbation of the equilateral triangle topology.

where the radars are arranged in a square topology of side length equal to R_{sp}. We leave it to the reader to verify the following:

$$C(h) = 100 \times \begin{cases} \frac{\pi s_h^2}{R_{sp}^2} & 0 \le s_h < \frac{R_{sp}}{2} \\ \frac{\pi s_h^2 - 2 s_h^2(\phi - \sin\phi)}{R_{sp}^2} & \frac{R_{sp}}{2} \le s_h < \frac{R_{sp}}{\sqrt{3}} \\ 1 & \frac{R_{sp}}{\sqrt{2}} \le s_h \end{cases} \quad (6)$$

and,

$$N_{CONUSradarcoverage} = \left(ceil\left[\frac{2843}{R_{sp}}\right] + 1 \right)^2 \quad (7)$$

In the above, ϕ is as defined in equation 4 and s_h is calculated as in equation 1 for the given value of h. Figure 6 plots the coverage and number of radars for a CONUS deployment as a function of spacing for radars arranged according to a square topology.

Comparing the square topology to the equilateral triangle topology, the two coverage floors (assuming $\theta_{min} = 0.9^o$, which is 1/2 the beam width of the mechanically scanned radars in the CASA IP1 testbed network), number of radars, and the total number of PAR panels for a CONUS deployment are shown in Table 1.

Topology	h_{floor} (m)	N_{radars}	# of Panels
Triangle	290 meters	10656	31968
Square	360 meters	9276	37104

Table 1: Comparison of Square Topology to Triangular Topology for a CONUS Deployment

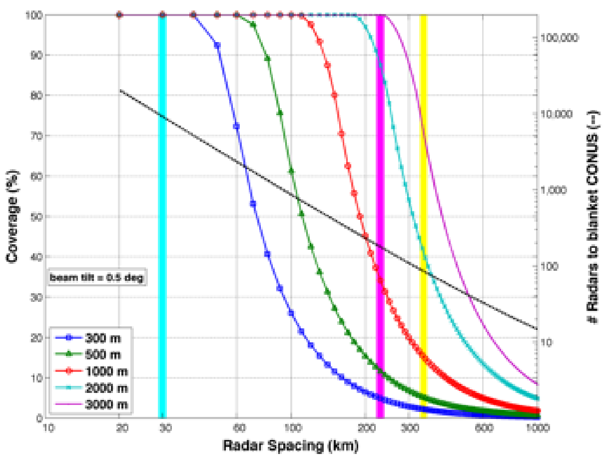

Figure 6: Coverage and number of radars plot for square topology.

It is seen that while fewer radars are required for CONUS coverage under the square topology than under the triangle topology, its low-altitude coverage has degraded, simply because it is less densely packed than the triangle topology. The desirability of one topology over the other will thus come from its impact on phased-array beam steering related degradation and total system cost.

5. Summary

For the idealized condition of a smooth earth, this paper presented an analysis connecting the density of a network of ground-based radars to the low-level coverage properties of the network. The main result was the presentation of the mathematical formulas leading to Figure 1, which illustrates the fundamental fact that the only way to improve low-altitude coverage is to place the radars very close together. For a CASA-type radar, which is defined as one with maximum range, R_{max} = 40 km, arranged in a network with spacing, R_{sp} = 30 km, between radars, this leads to an approximate 60:1 increase in the number of radars over the current NEXRAD-type radars (defined by, R_{max} = 230 km, arranged with spacing, R_{sp} = 230 km, between radars). The coverage floor, however, is reduced from 2500 m for NEXRAD to 290 m for CASA; a reduction that gives CASA a significant advantage in its ability to probe the lowest reaches of the atmospheric boundary layer (see also McLaughlin et al. (2009) and the references therein). As preliminary to identifying the optimal deployment of radars based on phased-array radar technology, the coverage equations for a topology based on square unit cells were also presented. It was discussed that while any perturbation away from the uniform equilateral triangle topology will degrade low-altitude coverage performance and may increase the total number of panels, the perturbation can have the advantage of reducing the required amount of beam steering, leading to less beam steering related performance degradation. A completion of that study is the subject of our on-going work as the CASA ERC prepares to deploy its phase-tilt (electronically scanned in azimuth, mechanically in elevation) research prototype radar (Hopf et al. (2009)).

References

Brewster, K., L. White, B. Johnson, and J. Brotzge, 2005: Selecting the sites for casa netrad, a collaborative radar network. *Ninth Symposium on Integrated Observing and Assimilation Systems for the Atmosphere, Oceans, and Land Surface*, **11.3**.

Doviak, R. J. and D. S. Zrnić, 1993: *Doppler Radar and Weather Observations*. Academic Press, 2 edition.

Hopf, A., E. Knapp, and D. McLaughlin, 2008: Scalable multifunction dense radar network. IEEE International Symposium on Geoscience and Remote Sensing, volume 4, 1018–1021.

Hopf, A., J. L. Salazar, R. Medina, V. Venkatesh, E. J. Knapp, S. J. Frasier, and D. J. McLaughlin, 2009: Casa phased array radar system description, simulation and products. IEEE International Symposium on Geoscience and Remote Sensing, volume 4.

Leone, D. A., R. M. Endlich, J. Petrieks, R. T. H. Collis, and J. R. Porter, 1989: Meteorological considerations used in planning the nexrad network. *Bulletin of the American Meteorological Society*, **70**.

Liu, Y., V. C. Y. Wang, D. Willie, and V. N. Bringi, 2007: Operational evaluation of the real-time attenuation correction system for casa ip1 testbed. *AMS, 33rd Conference on Radar Meteorology*.

Mailloux, R. J., 2005: *Phased Array Antenna Handbook*. Artech House, Norwood, MA, 2nd edition.

McLaughlin, D., V. Chandrasekar, K. Droegemeier, S. Frasier, J. Kurose, F. Junyent, B. Philips, S. Cruz-Pol, and J. Colom, 2005: Distributed collaborative adaptive sensing (dcas) for improved detection, understanding, and prediction of atmospheric hazards. 9th Symp. Integrated Obs. Assim. Systems - Atmos. Oceans, Land Surface (IOAS-AOLS), Amer. Meteor. Soc., San Diego, CA.

McLaughlin, D., D. Pepyne, V. Chandrasekar, B. Philips, J. Kurose, M. Zink, K. Droegemeier, S. Cruz-Pol, F. Junyent, J. Brotzge, D. Westbrook, N. Bharadwaj, Y. Wang, E. Lyons, K. Hondl, Y. Liu, E. Knapp, M. Xue, A. Hopf, K. Kloesel, A. DeFonzo, P. Kollias, K. Brewster, R. Contreras, T. Djaferis, E. Insanic, S. Frasier, and F. Carr, 2009: Short-wavelength technology and the potential for distributed networks of small radar systems. *Bulletin of the American Meteorological Society*, **preprint**, 0000–0000.

(NRC), N. R. C., 2002: *Weather Technology Beyond NEXRAD*. National Academy Press, Washington DC.

Salazar, J. L. and D. J. McLaughlin, 2007: Antenna design tradeoffs for dense distributed radar network for weather sensing.

Salazar, J. L., R. Medina, E. J. Knapp, and D. J. McLaughlin, 2008: Phase-tilt array antenna design for dense distributed radar network for weather sensing. IEEE International Symposium on Geoscience and Remote Sensing, Boston, MA.

Wang, Y., V. Chandrasekar, and B. Dolan, 2008: Development of scan strategy for dual doppler retrieval in a networked radar system. *Geoscience and Remote Sensing Symposium, 2008. IGARSS 2008. IEEE International*, volume 5, V –322–V –325.

Wang, Y., V. Chandrasekar, and D. J. McLaughlin, 2005: Antenna system requirement for dual polarization radar design in hybrid mode of operation. *32nd Conference on Radar Meteorology*.

Zhang, G., R. Doviak, D. Zrnic, and J. Crain, 2008: Phased array radar polarimetry for weather sensing: Challenges and opportunities. *Geoscience and Remote Sensing Symposium, 2008. IGARSS 2008. IEEE International*, volume 5, V –449–V –452.